Electronic Supplementary Information

The First Lead Fluorooxoborate PbB_5O_8F: Achieving the Coexistence of Large Birefringence and Deep-Ultraviolet Cutoff Edge

Miriding Mutailipu,[†,‡,+] Min Zhang,[†,+] Bingbing Zhang[†,‡] Zhihua Yang[†], and Shilie Pan[*,†]

†CAS Key Laboratory of Functional Materials and Devices for Special Environments; Xinjiang Technical Institute of Physics & Chemistry, CAS; Xinjiang Key Laboratory of Electronic Information Materials and Devices, 40-1 South Beijing Road, Urumqi 830011,China

‡University of Chinese Academy of Sciences, Beijing 100049, China

*Corresponding author, E-mail: slpan@ms.xjb.ac.cn

Experimental Section

Synthesis of PbB_5O_8F. Single crystals of PbB_5O_8F were grown by high-temperature solution method using a $NaBF_4$ flux in a closed system. A mixture of PbF_2 (0.1962 g, 0.8 mmol), $NaBF_4$ (0.1757 g, 1.6 mmol), and B_2O_3 (0.1114 g, 1.6 mmol) were loaded into a tidy silica glass tube (Φ10 mm × 100 mm) and dried in high-temperature to remove the inside impurities, and the tube was flame-sealed under 10^{-3} Pa. The tube was heated to 600 °C in 12 h, and held at this temperature for 48 h, and then cooled to 30 °C with a rate of 1.0 °C /h. Powder XRD analysis confirmed the phase purity.

Characterization. Powder XRD data were collected with a Bruker D2 PHASER diffractometer (Cu Kα radiation with λ = 1.5418 Å, 2θ = 10 to 60°, scan step width = 0.02°, and counting time= 1 s/step). The single-crystal XRD data were collected on a Bruker SMART APEX II 4K CCD diffractometer using Mo Kα radiation (λ = 0.71073 Å) at room temperature. Data integration, cell refinement and absorption corrections were carried out with the program SAINT.[1] The structure was solved by direct methods and refined on F^2 by full-matrix least-squares techniques using the program suite SHELXTL.[2] Solutions were checked for missed symmetry using PLATON.[3] Thermal gravimetric analysis (TGA) and differential scanning calorimetry (DSC) were carried out on a simultaneous NETZSCH STA 449 F3 thermal analyzer instrument in a flowing N_2 atmosphere, the sample was placed in Pt crucible, heated from 40 to 750 °C at a rate of 5 °C min^{-1}. Infrared spectroscopy was carried out on a Shimadzu IR Affinity-1 Fourier transform infrared spectrometer in the 400-4000 cm^{-1} range. UV−vis−NIR diffuse-reflectance spectroscopy data in the wavelength range of 190–2600 nm were recorded at room temperature using a powder sample of PbB_5O_8F on a Shimadzu SolidSpec-3700DUV spectrophotometer.

Computational methods. The electronic structure as well as optical property calculations was performed by employing CASTEP,[4] a plane-wave pseudopotential DFT package, with the norm-conserving pseudopotentials (NCP).[5] The Perdew-Burke-Emzerhof (PBE) functional within the generalized gradient approximation (GGA) was used.[6] The following orbital electrons were treated as valence electrons, Pb: $5d^{10}$ $6s^2$ $6p^2$, B: $2s^2$ $2p^1$, O: $2s^2$ $2p^4$, F: $2s^2$ $2p^5$. The plane-wave energy cutoff was

set at 940.0 eV. Self-consistent field (SCF) calculations were performed with a convergence criterion of 5×10^{-7} eV/atom on the total energy. The k-point separation for each material was set as 0.03 $Å^{-1}$ in the Brillouin zone corresponding to primitive cell, resulting in Monkhorst-Pack k-point meshes of 3 × 4 × 2. We kept the default values of the CASTEP code on the aspect of the other calculation parameters and convergent criteria.

Table S1. Crystal data and structure refinements of PbB_5O_8F.

Empirical formula	PbB_5O_8F
Formula weight	408.24
Wavelength (Å)	0.71073
Temperature (K)	296(2)
Crystal system	Orthorhombic
Space group	*Pbca*
a(Å)	10.885(3)
b(Å)	9.108(2)
c (Å)	13.576(3)
Z	8
Volume ($Å^3$)	1345.9(6)
Density (calc.) (g/cm^3)	2.938
Absorption coefficient (mm^{-1})	25.11
F(000)	1440
Crystal size (mm^3)	0.15×0.12×0.09
Theta range for data collection	3.00 to 27.53
Limiting indices	$-11 \le h \le 14, -11 \le k \le 11, -16 \le l \le 17$
Reflections collected / unique	7621 / 1550 [R(int) = 0.0417]
Completeness	99.9%
Data / restraints / parameters	1550/0/137
Goodness-of-fit on F^2	1.017
Final R indices [I>2sigma(I)][a]	$R_1 = 0.0218$, $wR_2 = 0.0444$
R indices (all data)[a]	$R_1 = 0.0323$, $wR_2 = 0.0481$
Extinction coefficient	0.00022 (5)
Largest diff. peak and hole ($e/Å^3$)	0.901 and -0.804

[a] $R_1 = \Sigma||F_o| - |F_c||/\Sigma|F_o|$ and $wR_2 = [\Sigma w(F_o^2 - F_c^2)^2/ \Sigma wF_o^4]^{1/2}$ for $F_o^2 > 2\sigma(F_o^2)$.

Table S2. Atomic coordinates equivalent isotropic displacement parameters and bond valence sum (BVS) for PbB_5O_8F.

Atoms	*x*	*y*	*z*	U_{eq}(Å^2)	BVS
Pb(1)	0.0384(1)	0.6800(1)	0.8852(1)	0.015(1)	1.874
B(1)	-0.2714(6)	0.7906(6)	0.9062(5)	0.012(1)	2.996
B(2)	-0.0092(6)	0.3457(6)	0.8678(5)	0.009(1)	3.043
B(3)	0.3025(5)	0.8739(6)	0.9575(5)	0.009(1)	3.081
B(4)	0.3302(5)	0.6975(6)	0.8212(5)	0.010(1)	3.029
B(5)	-0.3149(5)	0.9729(6)	0.7871(5)	0.011(1)	3.065
O(1)	0.0488(3)	0.2256(4)	0.8129(3)	0.011(1)	1.838
O(2)	0.2535(3)	0.7755(4)	0.8804(3)	0.012(1)	2.128
O(3)	-0.1836(3)	0.7065(4)	0.9497(3)	0.012(1)	2.087
O(4)	0.0775(3)	0.4269(4)	0.9283(3)	0.011(1)	2.053
O(5)	-0.2321(3)	0.8820(4)	0.8307(3)	0.011(1)	1.988
O(6)	-0.1074(3)	0.2843(4)	0.9323(3)	0.012(1)	1.995
O(7)	0.2692(3)	0.5896(3)	0.7668(3)	0.010(1)	1.903
O(8)	-0.0632(3)	0.4532(4)	0.7986(3)	0.012(1)	2.064
F(1)	0.2212(3)	0.9904(3)	0.9688(2)	0.015(1)	0.745

Table S3. Anisotropic displacement parameters ($Å^2$) for PbB_5O_8F.

Atom	U_{11}	U_{22}	U_{33}	U_{23}	U_{13}	U_{12}
Pb(1)	0.011(1)	0.015(1)	0.020(1)	0.001(1)	0.000(1)	-0.002(1)
B(1)	0.011(3)	0.012(3)	0.011(4)	0.000(2)	0.000(2)	-0.002(2)
B(2)	0.011(3)	0.011(3)	0.006(3)	-0.001(2)	0.002(2)	0.004(2)
B(3)	0.008(3)	0.011(3)	0.009(3)	0.000(2)	0.003(2)	0.000(2)
B(4)	0.011(3)	0.007(3)	0.012(3)	0.003(2)	0.000(2)	-0.002(2)
B(5)	0.011(3)	0.013(3)	0.008(3)	-0.002(3)	0.003(2)	-0.001(2)
O(1)	0.008(2)	0.014(2)	0.010(2)	-0.005(2)	-0.002(2)	0.001(1)
O(2)	0.009(2)	0.014(2)	0.012(2)	-0.004(2)	0.000(2)	-0.003(1)
O(3)	0.008(2)	0.019(2)	0.011(2)	0.002(2)	0.002(2)	0.004(1)
O(4)	0.008(2)	0.012(2)	0.013(2)	-0.002(2)	-0.005(2)	0.005(1)
O(5)	0.009(2)	0.014(2)	0.012(2)	0.004(2)	0.002(2)	0.003(1)
O(6)	0.009(2)	0.013(2)	0.013(2)	0.007(2)	0.003(2)	0.000(1)
O(7)	0.007(2)	0.009(2)	0.016(2)	-0.003(2)	0.002(2)	-0.002(1)
O(8)	0.008(2)	0.015(2)	0.015(2)	0.008(2)	0.001(2)	-0.001(1)
F(1)	0.016(2)	0.009(1)	0.020(2)	0.000(1)	0.001(1)	0.006(1)

Table S4. Selected bond lengths (Å) and angles (°) for PbB_5O_8F.

Bond lengths		Bond angles	
Pb(1)-O(4)	2.416(3)	O(3)-B(1)-O(6)	122.9(5)
Pb(1)-O(2)	2.499(4)	O(3)-B(1)-O(5)	116.2(5)
Pb(1)-O(3)	2.581(4)	O(6)-B(1)-O(5)	120.9(5)
Pb(1)-O(6)	2.609(4)	O(4)-B(2)-O(8)	106.3(4)
Pb(1)-O(8)	2.621(4)	O(4)-B(2)-O(6)	108.9(5)
Pb(1)-O(1)	2.882(3)	O(1)-B(2)-O(8)	110.0(4)
Pb(1)-O(4)	2.991(4)	O(1)-B(2)-O(6)	109.1(4)
Pb(1)-O(7)	3.094(3)	O(4)-B(2)-O(1)	112.7(4)
B(1)-O(3)	1.359(7)	O(8)-B(2)-O(6)	109.7(4)
B(1)-O(6)	1.366(7)	O(4)-B(3)-O(3)	108.0(4)
B(1)-O(5)	1.389(7)	O(4)-B(3)-O(2)	109.5(4)
B(2)-O(4)	1.454(7)	O(3)-B(3)-O(2)	110.1(4)
B(2)-O(1)	1.467(7)	O(1)-B(4)-O(2)	123.4(5)
B(2)-O(8)	1.478(7)	O(1)-B(4)-O(7)	123.7(5)
B(2)-O(6)	1.491(7)	O(2)-B(4)-O(7)	112.8(5)
B(3)-F(1)	1.390(6)	O(5)-B(5)-O(7)	117.4(5)
B(3)-O(4)	1.448(7)	O(8)-B(5)-O(5)	121.4(5)
B(3)-O(3)	1.465(7)	O(8)-B(5)-O(7)	121.2(5)
B(3)-O(2)	1.478(7)		
B(4)-O(1)	1.346(6)		
B(4)-O(2)	1.360(7)		
B(4)-O(7)	1.397(7)		

Figure S1. TG-DSC curves (a) and powder XRD patterns (b) of PbB_5O_8F.

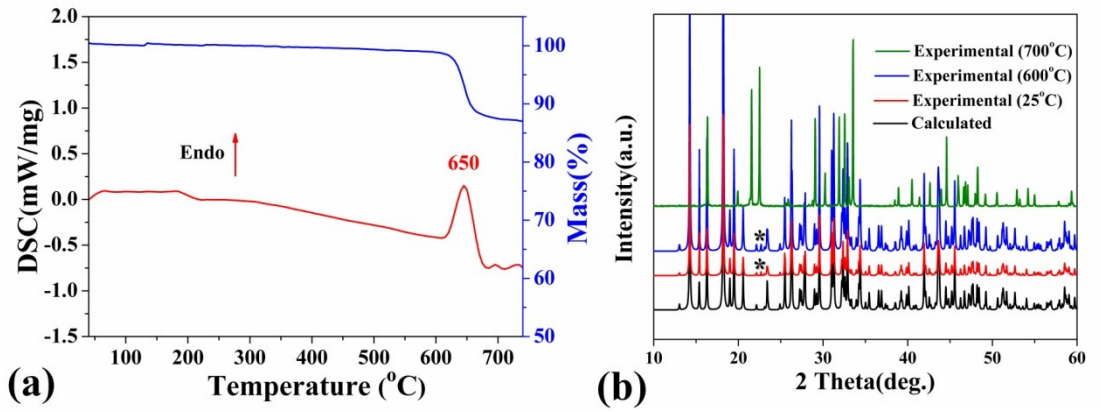

Figure S2. The structual evolution from $[B_5O_{11}]^{7-}$ (a) to $[B_5O_{10}F]^{6-}$ (b)

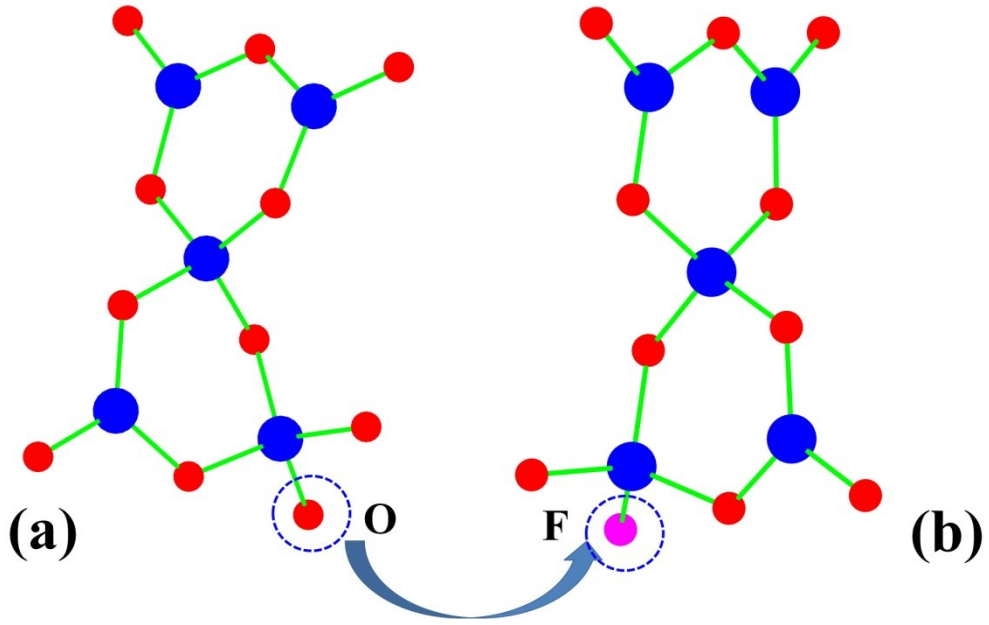

Figure S3. (a) The toplogical layered structures of PbB_5O_8F in which the $[B_5O_{10}F]^{6-}$ fundamental building blocks are considered as four-connected nodes. (b) Two interpenetrating 3D nets in $[B_5O_{10}F]^{6-}$.

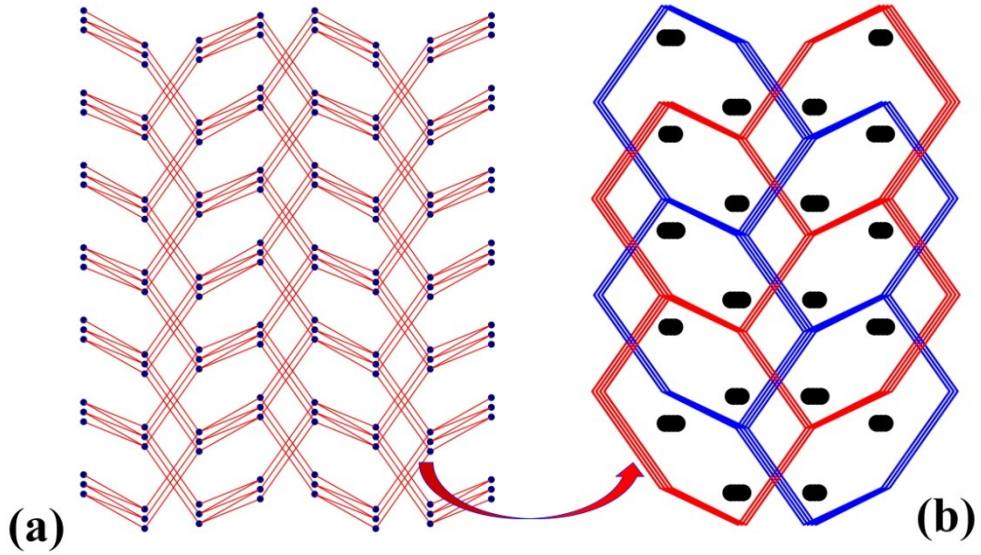

Figure S4. The infrared spectrum of PbB_5O_8F.

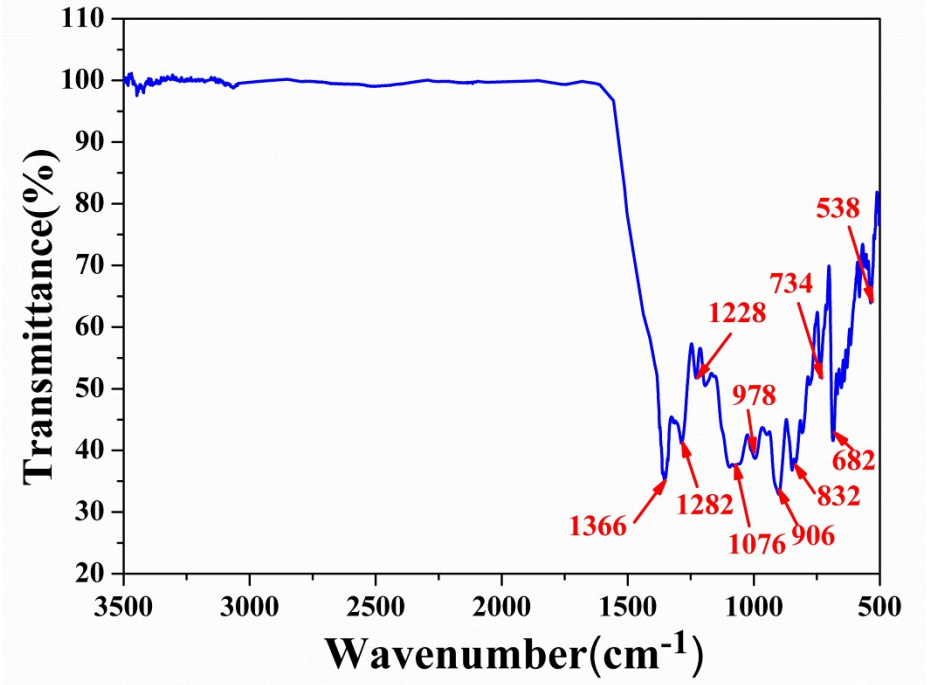

The infrared spectrum of PbB_5O_8F was also examined to specify the coordination model of the B atoms based on the data of previously reported borates.[7-10] The asymmetric and symmetric stretching of the $[BO_3]^{3-}$ groups are observed at 1366 and 978 cm^{-1}, respectively. The out-of-plane bending of the $[BO_3]^{3-}$ groups appears at 734 and 682 cm^{-1}. The peak at 538 cm^{-1} corresponds to the bending of the $[BO_3]^{3-}$ group. Specially, the asymmetric stretching of the B–F bond is found at 1282 cm^{-1}, and the symmetric out of phase stretching of the B–F bond is also found at 832 cm^{-1}, this further confirms the existence of the B-F bonds in the structure of PbB_5O_8F.

Figure S5. Electronic band structure of PbB_5O_8F based on the results of GGA method.

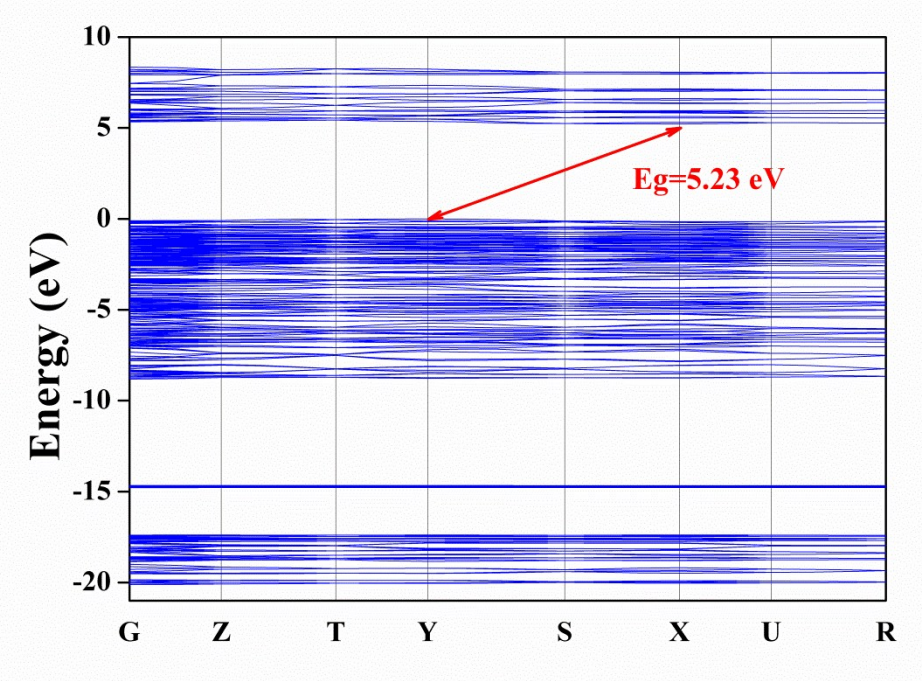

Figure S6. The projected and total density of states of PbB_5O_8F.

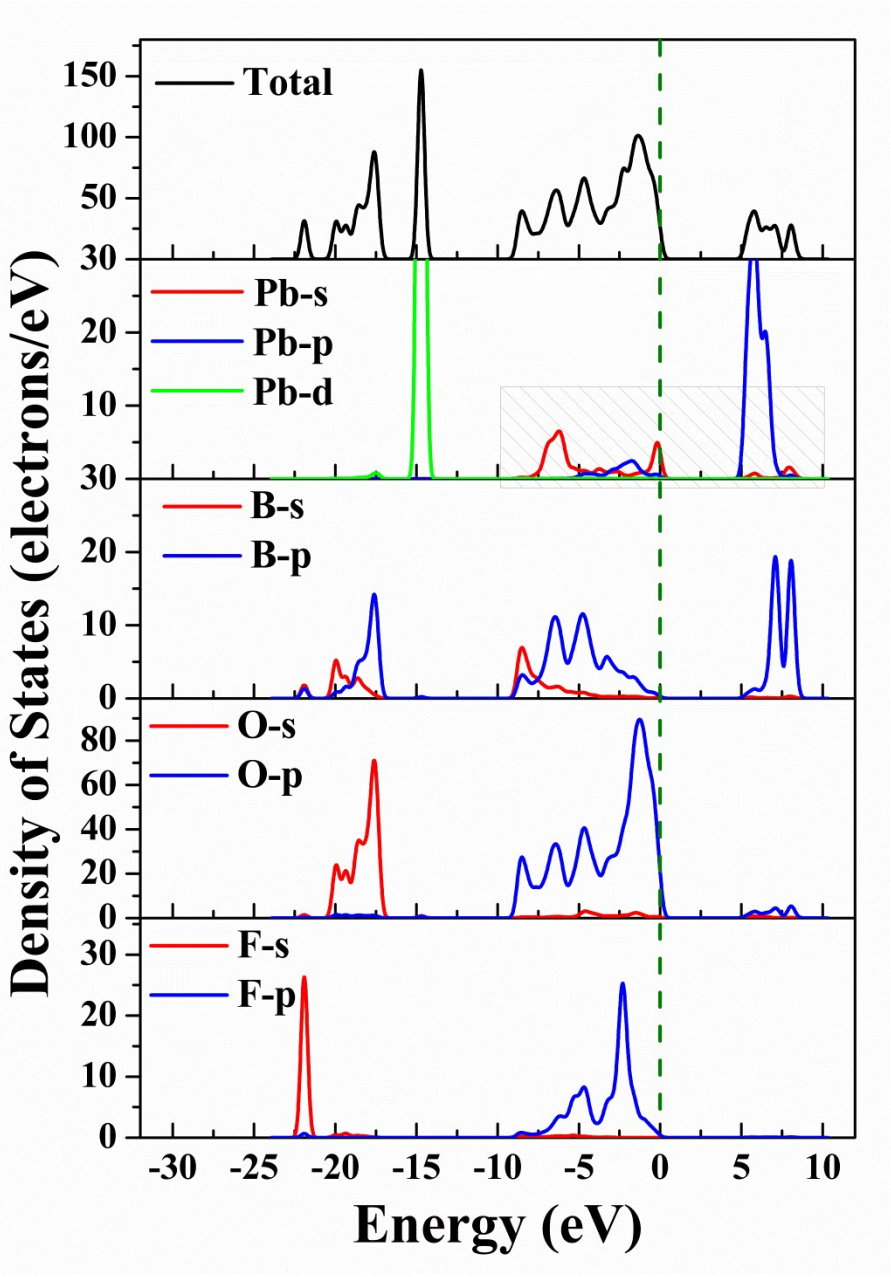

Figure S7. The electron localization function diagrams of in PbB_5O_8F sliced along the direction of (0.53, 0.70, 0.62).

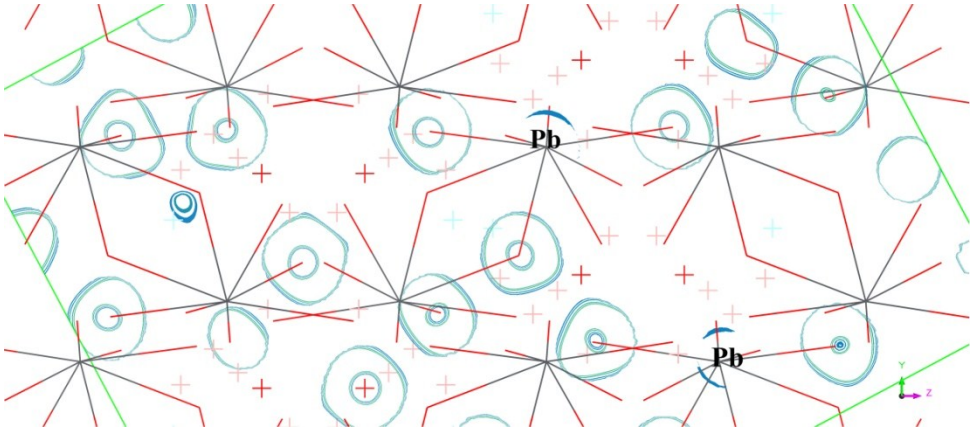

Figure S8. The electron localization function diagrams of PbB_5O_8F.

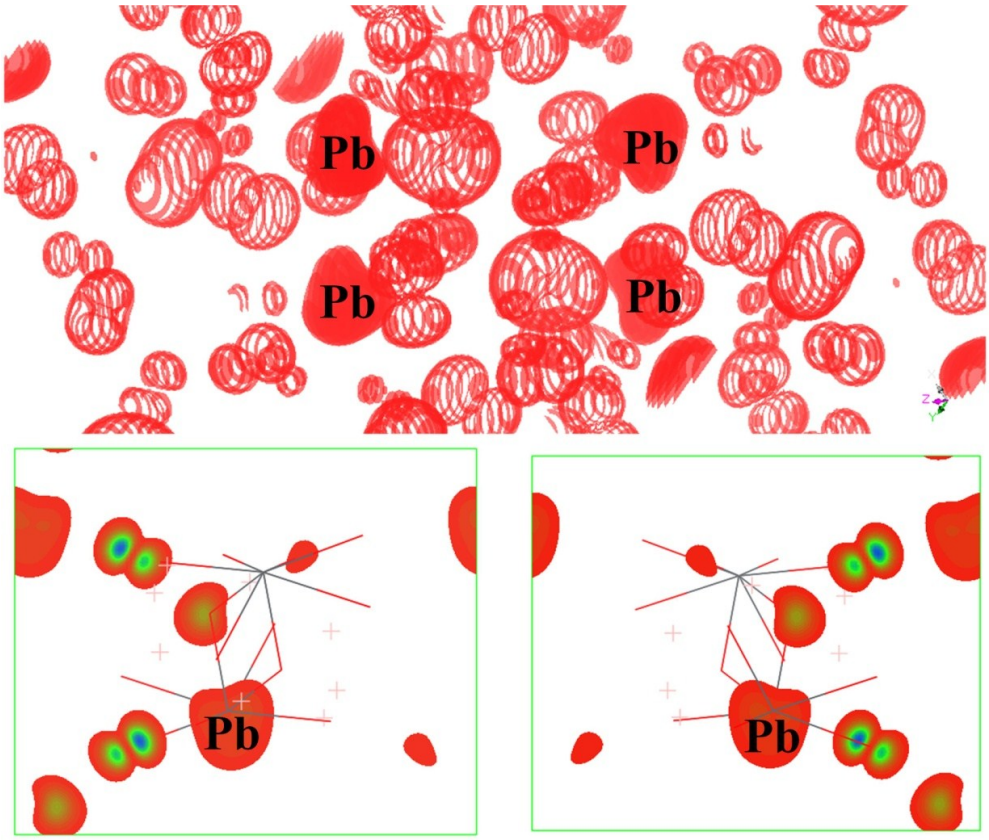

References and Notes

[1] SAINT, *Version 7.60A,Bruker Analytical X-ray Instruments, Inc.,Madison, WI,* 2008.

[2] G. M. Sheldrick, *SHELXTL, version 6.12; Bruker Analytical X-ray Instruments, Inc.: Madison, WI,* 2001.

[3] A. L. Spek, *J. Appl. Crystallogr.* 2003, **36**, 7.

[4] S. J. Clark, M. D. Segall, C. J. Pickard, P. J. Hasnip, M. J. Probert, K. Refson, M. C. Payne, *Z. Anorg. Allg. Chem.,* 2005, **220**, 567.

[5] a) A. M. Rappe, K. M. Rabe, E. Kaxiras, J. D. Joannopoulos, *Phys. Rev. B,* 1990, **41**, 1227; b) J. S. Lin, A. Qteish, M. C. Payne, V. Heine, *Phys. Rev. B,* 1993, **47**, 4174; c) M. H. Lee, PhD. Thesis, The University of Cambridge 1996.

[6] J. P. Perdew, K. Burke, M. Ernzerhof, *Phys. Rev. Lett.,* 1996, **77**, 3865.

[7] J. Li, S. Xia, S. Gao, *Spectrochim. Acta A* 1995, **51**, 519.

[8] S. D. Ross, In The Infrared Spectra of Minerals; Farmer, V. C., Ed.; Mineralogical Society of Great Britain and Ireland: Middlesex, U.K., 1974; 205.

[9] G. Q. Shi, Y. Wang, F. F. Zhang, B. B. Zhang, Z. H. Yang, X. L. Hou, S. L. Pan and K. R. Poeppelmeier, *J. Am. Chem. Soc.,* 2017, **139**, 10645.

[10] M. Mutailipu, M. Zhang, B. B. Zhang, L. Y. Wang, Z. H. Yang, X. Zhou and S. L. Pan, *Angew. Chem. Int. Ed.,* 2018, **DOI:** 10.1002/anie.201802058.